PCCP

Description of electrolyte effects on the kinetics of reactions between ions in solution, using the mean spherical approximation

Jean-Pierre Simonin* and Hendrawan Hendrawan

Laboratoire Liquides Ioniques et Interfaces Chargées (LI2C-UMR 7612), Université P.M. Curie, Boîte no. 51, 4 Place Jussieu, 75252 Paris Cedex 05, France. E-mail: sim@ccr.jussieu.fr

The effect of an inert salt on the kinetics of solution reactions between ions is examined in the framework of the mean spherical approximation (MSA) theory. The latter is applied to describe activation- and diffusion-controlled reactions in moderately concentrated electrolyte solutions. The results are compared with those obtained using the Debye–Hückel theory, in particular beyond the limit of applicability of this model. It is shown that both theories may be applied to represent salt effects with nearly equal accuracy.

1 Introduction

It is well known that solution reactions can be classified between two limiting cases. The first concerns reactions in which the chemical reaction step occurs very rapidly, virtually instantaneously, when the reactants encounter. These are known as diffusion-controlled reactions (DCRs). Here, the reaction rate constant is typically of the order of 10^{10} mol^{-1} dm^3 s^{-1}. The other class of reactions is represented by those in which the chemical reaction is slow as compared to the encounter process. This type of reaction is often called an activation-controlled reaction (ACR) because a high activation energy is needed to yield the products. Here, the rate constant is roughly of the order of 1 mol^{-1} dm^3 s^{-1}.

The influence of a salt on the kinetics of reactions between ions in solution has been the subject of many experimental and theoretical investigations. This type of study has played a determining role in the understanding of the mechanisms of solution reactions.

Thus, it was the study of salt effects on ion–ion ACR kinetics that first led Brönsted to introduce a new species, the "intermediate" or "activated" complex ion, formed by collision of the reactants.[1] In this model, the complex ion bears a charge that is the algebraic sum of the reactant charges. The theory was applied to interpret experimental results, by using expressions for the activity coefficients of the species. The latter were taken from the Debye–Hückel (DH) theory.[2] The treatment, and the results obtained therefrom, were summarised later by Livingston.[3]

The first description of the kinetics of DCRs between charged particles may be traced back to the pioneering work of Langevin[4] in 1903. However, the reference work is that of Debye,[5] published in 1942, which extended the classical description of Smoluchowski to the case of charged reactants. In Debye's paper, the DH theory[2] was used to provide a theoretical expression for the effective potential of mean force (PMF), modified by the added supporting electrolyte and in which the reactants diffuse toward each other. Kinetic electrolyte effects on DCRs between ions have been extensively studied experimentally. Typical examples are the quenching of fluorescence[6–14] and reactions involving the solvated electron.[15–18] The theory of Debye constitutes the basic framework in which experimental data may be interpreted.

A noticeable feature is that the expressions for the variation of the rate constant *vs.* added salt are identical[19] for both DCRs and ACRs at very low salt concentration, when using the DH limiting law (DHLL). Typically, for the representation of departures from ideality in electrolyte solutions, the DHLL is applicable to 10^{-2} mol dm^{-3} for a 1 : 1 salt in water. This limit is lower for polyvalent ions.

It may be noticed on a Livingston diagram[3] that it is for this typical value of the ionic strength that the values of the experimental rates begin to deviate from (and vary less rapidly than) the DHLL prediction.[19,20] A description of the experimental data at higher salt concentration was obtained by using the extended DH (EDH) expressions instead of the DHLL.[21] A more recent representation has been given,[22] in the framework of the mean spherical approximation[23–25] (MSA) model. In this work, the treatment was applied to some typical ACRs on the basis of the Brönsted relation, in which the activity coefficients of the reactants and of the activated complex were assessed using the MSA. A similar procedure has been used in another recent study.[26]

The MSA model is an interesting tool for the representation of ionic solution properties. In the DH theory, ions are represented by point charges that cannot approach a particular central ion by more than some distance; at the same time, no constraint is imposed on the relative distance between two ions in the cloud surrounding the central ion. In contrast, in the MSA model, ions are modeled as charged hard spheres. Thus, volume exclusion effects are better accounted for in the MSA than in the DH approach. Moreover, it provides analytical and rather simple expressions that have a striking similarity with the expressions derived from the DH theory.[27] The typical value of the maximum concentration, of a 1 : 1 salt in water, to which the basic MSA may be applied is 1 mol dm^{-3}, as compared to 0.1 mol dm^{-3} for the EDH expressions[28] and 0.01 mol dm^{-3} for the DHLL. On the other hand, the MSA has some well known deficiencies,[27] for which some solutions have been proposed. One of them, the exponential MSA (denoted here as EMSA), is used in this work. In the EMSA, the ion–ion radial distribution function (RDF) is accurate to at least 2 mol dm^{-3} for a 1 : 1 salt.[29]

In this work, the description of salt effects on solution reaction kinetics is re-examined in the framework of the MSA. One motivation for this study was our (future) intention of analysing new experimental data obtained for a DCR in a wider electrolyte concentration range. Noting that the DH framework is *a priori* not suited to concentrated solutions, it was realised that the MSA constitutes a viable approach.

Moreover, the MSA is the first way of studying the influence of the nature of the salt beyond the DH picture, in which the presence of a salt is characterised only by its ionic strength. In the MSA, besides its charge, the identity of an ion is distinguished by its diameter. In this work, the salt ions are supposed to have equal diameters. With this assumption, the effect of the nature of the salt could be studied using simpler formulas.

In the present paper, the description of salt effects on the kinetics of ACRs and DCRs is studied beyond the limit of applicability of the DH theory, using the MSA model, at the primitive level of ionic solutions. (The term 'primitive' means that the solvent is regarded as a continuum that manifests itself only through its dielectric permittivity. It is implicit henceforth that the solvent is water.) In each case, the results found using the EMSA are compared with those obtained using the EDH theory, in particular above the limit of validity of the latter. In the case of ACRs, the description is based on an expression involving the RDF between the reactants, which differs from the classic Brönsted treatment. This procedure leads to expressions that coincide with the classic DH expressions at low salt concentration and are simpler than previous ones[22] at the MSA level. In the case of DCRs, EDH and EMSA formulae are inserted into the fundamental equation of Debye, and numerical results are computed for typical systems. Moreover, an often-used formula is shown to be inaccurate in this context.

This paper is organised as follows. In the next section, expressions are given for the ion–ion PMF and RDF, which are basic quantities for the description of solution reaction kinetics at the level of the primitive model of solutions. These expressions are derived using the EDH and EMSA theories. They are used in the third section to derive formulae for the kinetics of ACRs and DCRs. Then, the corresponding results are presented and discussed in the last section.

2 Basic statistical mechanical relations

Expressions for the ion–ion PMF and RDF are given in this section.

We recall that, if V denotes the PMF, the RDF g is related to V through the relation

$$g(r) \equiv \exp[-\beta V(r)] \tag{1}$$

where $\beta \equiv (k_B T)^{-1}$ (k_B is the Boltzmann constant and T is the temperature).

We will designate the reactants by the symbols A and B, bearing charges $z_A e$ and $z_B e$, respectively, with e being the elementary charge.

2.1 Absence of salt

Let us consider infinitely dilute reactants, without added salt. Denoting by $V_{AB}^{(0)}$ the potential of mean force between the reactants in this case, the following equation (that has been used frequently, e.g. to test the influence of the solvent permittivity in the primitive model[19]) may be written

$$\beta V_{AB}^{(0)}(r) = \frac{\lambda_{AB}}{r} \tag{2}$$

in which we set for convenience

$$\lambda_{AB} \equiv z_A z_B \lambda \tag{3}$$

$$\lambda \equiv \beta e^2/(4\pi \varepsilon_0 \varepsilon_W) \tag{4}$$

with ε_0 being the permittivity of a vacuum.

Eqn. (2) expresses the classic Coulomb potential of mean force for two charges $z_A e$ and $z_B e$ separated by the center-to-center distance r in a medium of permittivity ε_W. Notice that λ is twice the Bjerrum critical distance for ion-pair formation.[28]

Then $g_{AB}^{(0)}(r)$, the RDF in the absence of salt, is found by inserting eqn. (2) into eqn. (1).

We now consider solutions composed of reactants A and B at trace concentrations in an inert salt solution. The latter is supposed to be a fully dissociated pure electrolyte. The + and − indices are used to designate the ions of the salt.

2.2 Results from DH theory

We now suppose that the solution contains added salt at a finite concentration.

For a sufficiently dilute supporting electrolyte, the potential of mean force between the reactants A and B, vs. the center-to-center distance r, may be expressed through the EDH relation[27,28]

$$\beta V_{AB}^{EDH}(r) = \frac{\lambda_{AB}}{r} \frac{\exp[-\kappa(r-\sigma)]}{1 + \kappa\sigma} \tag{5}$$

At the level of the DH theory, σ stands for the distance of closest approach between the centers of ions A and B. Besides, κ is the classic Debye screening parameter, verifying

$$\kappa^2 = 4\pi\lambda(\rho_+ z_+^2 + \rho_- z_-^2) \tag{6}$$

in which ρ_i is the number density of ion i (number of particles per volume unit) and z_i is its valence.

2.3 Results from MSA theory

The concentration of the salt will be supposed sufficiently low (typically below 1 or 2 mol dm^{-3}) so that the sizes of the ions and the solution permittivity may be taken as constant.

Here, we will assume that both ions of the salt have the same size, denoted by σ_S, that is

$$\sigma_+ = \sigma_- = \sigma_S \tag{7}$$

In the MSA framework, the thermodynamic properties of electrolytes may be well described using this assumption, as long as the solution is not too concentrated. The typical value of the ionic diameter is 4×10^{-10} m, as in a representation using the DH model.[28] Precise values of average ion sizes for the MSA treatment are given in Table 1 below, together with the concentration range allowed. On the other hand, the reactants may have arbitrary sizes σ_A and σ_B.

An advantage of eqn. (7) is that it simplifies greatly the MSA formulas. So, the screening parameter Γ[30] is given by

$$\Gamma = \frac{\sqrt{1 + 2\kappa\sigma_S} - 1}{2\sigma_S} = \kappa(1 + \sqrt{1 + 2\kappa\sigma_S})^{-1} \tag{8}$$

From this equation one finds that $2\Gamma < \kappa$ for a finite salt concentration, and $2\Gamma \simeq \kappa$ when the salt concentration is very small. Therefore, defining the MSA and DH screening lengths as $l_{MSA} = 1/(2\Gamma)$ and $l_{DH} = 1/\kappa$, it follows that

$$l_{MSA} > l_{DH}$$

which may be regarded as a consequence of the fact that, as stated in the Introduction, the MSA accounts for excluded volume effects better than does the DH model.

Let us notice that the screening parameters differ appreciably for typical ionic solutions. So, the value of the relative difference $(2\Gamma - \kappa)/\kappa$ is 6%, 15% and 31% in solutions of 0.01, 0.1 and 1 mol dm^{-3} ionic strength, respectively, for an electrolyte in which both ions have a diameter of 4×10^{-10} m.

There is another interesting consequence that can be drawn from eqn. (8). Generally in the MSA, the characteristics of an electrolyte solution are the salt concentration, and the sizes and charges of the ions. In the present case of eqn. (7), Γ is a function of κ and σ_S alone. Besides, as shown through eqn. (26) below, κ is proportional to $I^{1/2}$. Therefore, Γ will be a function of I and σ_S. This feature has the important conse-

quence that, in this version of the MSA, the nature of a (non-associating) salt will be characterised solely by the common ion size σ_S.

We now present the ingredients for expressing the RDF in the EMSA. Then, we give formulae for the contact value of the RDF and, lastly, the expression of the RDF as a function of interparticle separation. The latter case requires more extensive calculations.

2.3.1 Exponential expression for the RDF in the MSA.
The pair distribution function in the MSA is of the form[30]

$$g^{MSA}(r) = g^{HS}(r) + g^{el}(r) \qquad (9)$$

where g^{HS} is the hard sphere (HS) part of the pair distribution function (taking all ions as neutral particles) and g^{el} is the electrostatic part.

The radial distribution function in the MSA (eqn. (9)) is known to be significantly inaccurate.[27] Nevertheless, an accurate equation[27] for g may be obtained using the exponential approximation,[29,31,32] which reads

$$g^{EMSA} \simeq g^{HS} \exp(g^{el}) \qquad (10)$$

In the remainder of this work, we will take $g^{HS} = 1$ even in presence of ions of the added salt. This choice is not consistent with the framework adopted for the present treatment, developed at the primitive level of solutions (which should entail $g^{HS} > 1$). However, noting that g^{HS} is not evaluated realistically at this level because the solvent is not taken into account, we prefer to assume that the excluded volume contribution to the RDF is not modified by salt addition ($g^{HS} = 1$ in absence of salt). Thus, we assume that electrostatic effects govern the variation of the RDF.

Then, using eqn. (10) in eqn. (1), we get

$$\beta V^{EMSA} \simeq -g^{el} \qquad (11)$$

Moreover, one notices that, contrary to the combination of eqn. (1) and (9), one recovers eqn. (2) from eqn. (11) and (20) below for vanishingly small salt concentration. Moreover, eqn. (11) and (12) lead to the same result as eqn. (5) for the PMF at contact, for low salt concentration. This can be shown by replacing Γ by $\kappa/2$ in eqn. (12).

2.3.2 Contact value of the RDF.
The electrostatic part of the contact value of the RDF in eqn. (9) is given by the following simple formula[30]

$$g^{el}(\sigma) = -\lambda z'_A z'_B / \sigma \qquad (12)$$

where, because of eqn. (7), one has

$$z'_i \equiv z_i/(1 + \Gamma \sigma_i) \qquad (13)$$

with σ_i the diameter of ion i and

$$\sigma \equiv (\sigma_A + \sigma_B)/2 \qquad (14)$$

2.3.3 RDF as a function of interionic distance.
Here, we compute the RDF and PMF in the MSA as a function of r, the distance between the centers of reactants A and B.

We introduce first the function

$$G(r) \equiv r g^{el}_{AB}(r) \qquad (15)$$

and the Laplace transform of G

$$\tilde{G} \equiv \int_0^\infty G(r)\exp(-sr)\,dr \qquad (16)$$

A general expression for this quantity has been found elsewhere.[30] After some simplifications, in which we use eqn. (7) and the fact that $\rho_A = \rho_B = 0$ (trace amounts of the reactants),

we obtain

$$\tilde{G} = \exp(-s\sigma_{AB})\tilde{F} \qquad (17)$$

with

$$\tilde{F} = -sA_{AB}/[s^2 + 2\Gamma s + 2\Gamma^2[1 - \exp(-s\sigma_S)]]$$

$$A_{AB} \equiv \frac{\lambda_{AB}}{(1 + \Gamma\sigma_A)(1 + \Gamma\sigma_B)} \qquad (18)$$

The term $\exp(-s\sigma_{AB})$ is put apart in eqn. (17) because it simply introduces translation[33] in the original function of $\tilde{F}$.

Inversion of $\tilde{F}$ in eqn. (18) is performed as follows. First it may be written in more compact form by introducing the non-dimensional parameters $s' \equiv s\sigma_S$ and $\Gamma' \equiv \Gamma\sigma_S$, which yields

$$\tilde{F} = -s'\sigma_S A_{AB}/[s'^2 + 2\Gamma's' + 2\Gamma'^2(1 - \exp(-s'))]$$

Inversion of this expression can be performed using the procedure of Henderson et al.[34] By making the change of variable $r' \equiv r/\sigma_S$ in eqn. (16), one finally arrives at

$$G(r) = -A_{AB} \sum_{n=1}^\infty G_n(x_n)H(r - \sigma_n) \qquad (19)$$

where

$$\sigma_n = \sigma + (n - 1)\sigma_S$$

$$x_n = \Gamma(r - \sigma_n)$$

$$G_n(x) = e^{-x} \frac{x^n}{(n-1)!}\left[j_{n-2}(x) - j_{n-1}(x)\right]$$

H is the Heaviside step function ($H(x) = 1$ for $x \geqslant 0$, $H(x) = 0$ for $x < 0$) and j is the spherical Bessel function of the first kind. The latter can easily be computed from an iterative procedure,[33] for instance by using the symbolic computation system Maple™. This yields

$$j_0(x) = \sin x/x$$

$$j_1(x) = \sin x/x^2 - \cos x/x$$

$$j_2(x) = (3/x^3 - 1/x)\sin x - 3\cos x/x^2$$

$$j_3(x) = (15/x^4 - 6/x^2)\sin x + (-15/x^3 + 1/x)\cos x$$

$$\cdots$$

Further,

$$G_1(x) = e^{-x}(\cos x - \sin x)$$

Therefore, we get the PMF from eqn. (11), (15) and (19) as

$$\beta V^{EMSA}_{AB}(r) = \frac{\lambda_{AB}}{r} \frac{1}{(1 + \Gamma\sigma_A)(1 + \Gamma\sigma_B)}$$

$$\times \sum_{n=1}^\infty G_n(x_n)H(r - \sigma_n) \qquad (20)$$

which shows similarity with eqn. (5).

The RDF $g^{el}_{AB}(r)$ is obtained by inserting eqn. (20) into eqn. (1).

3 Application to the kinetics of reactions

3.1 ACRs

3.1.1 Fundamental relations.
The fundamental equation suggested by Brönsted is that the rate "constant" k for a reaction between ionic species A and B may be expressed as

$$\frac{k}{k_0} = \frac{\gamma_A \gamma_B}{\gamma_X} \qquad (21)$$

in which γ_i is the activity coefficient of species i, X is the activated complex and k_0 is the rate constant without salt (the

reference state for activity coefficients). Eqn. (21) was justified subsequently by Bjerrum[35] who emphasised the determinant role of the activated complex concentration.

An alternative description is based on the relation

$$k = k_R \, g_{AB}(\sigma_R) \qquad (22)$$

in which σ_R represents the center-to-center distance between the reactants A and B, at which the reaction may proceed. This is a simplified relation (the full relation[36] involves a continuous set of reaction distances), but its form is appropriate to the present study. In eqn. (22), k_R is a characteristic parameter for the 'intrinsic' reaction.

Eqn. (22) is classic in the chemical kinetics theory of activated processes[19,37] and it is common in modern theory, e.g. in ref. 36. For the present purpose, it expresses in a simple and compact manner the effect of the supporting medium on the kinetics. In particular, it states that the kinetic rate is proportional to the "probability" that the two ions are at the distance σ_R, the reaction distance.

In this study we will suppose that σ_R coincides with the closest approach distance, that is

$$\sigma_R = \sigma$$

For the effect of a salt, one may derive the following equations. From eqn. (22), and supposing that the reaction distance σ, and the rate k_R, are not modified by addition of salt (which assumption may be valid for solutions of low to moderate ionic strength), one obtains the following relation

$$\frac{k}{k_0} = \frac{g_{AB}(\sigma)}{g_{AB}^{(0)}(\sigma)} \qquad (23)$$

instead of eqn. (21).

Eqn. (23) has the advantage over eqn. (21) that it involves only a property for the reactants. The computation of a quantity for a third species (the activity coefficient of X in the Brönsted equation, eqn. (21) is not required. As seen below, this feature leads to simpler formulae. At the primitive level of solutions, the use of eqn. (23) is justified by the fact that the solutions studied here are moderately concentrated. In the opposite case, one may expect that the species X should have to be taken into account explicitly, e.g. by ascribing a suitable size to it. Further, let us mention that eqn. (23) is identical[38] to eqn. (21) if the ratio $\gamma_A \gamma_B / \gamma_X$ is expressed using the binding MSA.[39]

Eqn. (23) is now applied to ACRs at the classic level[35] of the primitive model for solutions, in which the solvent (water) is regarded as a continuum of relative permittivity ε_W.

3.1.2 Results in the DH approximation. We obtain from eqn. (1)–(3), (5) and (23),

$$\ln(k/k_0)^{EDH} = \lambda_{AB} \kappa / (1 + \kappa\sigma) \qquad (24)$$

For low salt concentrations, such that $\kappa\sigma \ll 1$, we get the Brönsted formula in the form

$$\ln(k/k_0)^{DHLL} \simeq \lambda_{AB} \kappa \qquad (25)$$

The classic form of this equation can be recovered by introducing the ionic strength

$$I \equiv \frac{1}{2} \sum_{k = +, \, -} C_k z_k^2$$

in which C_k is the molar concentration of ion k. Then, it is easy to show that, with the present notations,

$$\kappa = 2\sqrt{2\pi \mathcal{N} \lambda} \sqrt{I} \qquad (26)$$

with $\mathcal{N}$ the Avogadro number and, using eqn. (26), eqn. (25) may be rewritten as

$$\log_{10}(k/k_0)^{DHLL} = 2A^{DH} z_A z_B \sqrt{I} \qquad (27)$$

which is the equation derived by Brönsted using the DHLL,[1] with

$$A^{DH} \equiv (2\pi \mathcal{N} \lambda^3)^{1/2} / \ln(10) \qquad (28)$$

At 25 °C, the value of A^{DH} is 0.51 if C is in mol dm^{-3} and that of λ is ca. 7×10^{-10} m.

For greater salt concentrations (for which the condition $\kappa\sigma \ll 1$ is not fulfilled) we have

$$\log_{10}(k/k_0)^{EDH} = 2A^{DH} z_A z_B \sqrt{I} / (1 + \kappa\sigma) \qquad (29)$$

instead of eqn. (27).

This equation was introduced by Scatchard.[21] In passing, one notices that, contrary to the latter work, no difficulty is encountered here with the size to attribute to X.

3.1.3 Results in the MSA. By combining eqn. (1), (2), (11), (12) and (23), we obtain

$$\ln(k/k_0)^{EMSA} = \frac{\lambda_{AB}}{\sigma} \left[1 - \frac{1}{(1 + \Gamma\sigma_A)(1 + \Gamma\sigma_B)} \right] \qquad (30)$$

It can be checked that this equation yields the classic result of Brönsted when the salt concentration is very small. In this case, $\Gamma \simeq \kappa/2$. Then, a first-order series expansion of eqn. (30) for κ leads to eqn. (25).

Particular cases. Case $\sigma_B = 0$. A particular form of eqn. (30) is obtained in the limiting case of complete size asymmetry for the reactants, e.g. $\sigma_B = 0$. Then, $\sigma_A = 2\sigma$ because of eqn. (14) and in this particular case we obtain from eqn. (30)

$$\ln(k/k_0)^{EMSA} = \frac{2\lambda_{AB} \Gamma}{(1 + 2\Gamma\sigma)} \qquad (31)$$

which is similar to eqn. (24) with 2Γ replacing κ.

Restricted case. In the restricted case (denoted by index r) where

$$\sigma_A = \sigma_B = \sigma$$

eqn. (30) yields

$$\ln(k/k_0)_r^{EMSA} = 2\lambda_{AB} \Gamma \frac{1 + \Gamma\sigma/2}{(1 + \Gamma\sigma)^2} \qquad (32)$$

from which one gets, using eqn. (8), and (24)

$$\ln(k/k_0)_r^{EMSA} = \ln(k/k_0)^{EDH}$$
$$\times \frac{(1 + \Gamma\sigma/2)[(1 + \Gamma\sigma)^2 + \Gamma^2\sigma(2\sigma_S - \sigma)]}{(1 + \Gamma\sigma_S)(1 + \Gamma\sigma)^2} \qquad (33)$$

with Γ given by eqn. (8).

3.2 DCRs

3.2.1 General relations. We use the result found by Debye for the rate constant in this case

$$k = 4\pi(D_A + D_B)L \qquad (34)$$

in which D_A and D_B are the diffusion coefficients of A and B, and L has the dimension of a length and is given by the following equation

$$L^{-1} = \int_{\sigma_R}^{\infty} \frac{\exp[\beta V_{AB}(r)]}{r^2} \, dr \qquad (35)$$

In this relation, σ_R is the distance at which the reaction occurs, and V_{AB} is the PMF. Using eqn. (1), eqn. (35) may be rewritten as

$$L^{-1} = \int_{\sigma_R}^{\infty} \frac{1}{r^2 g_{AB}(r)} \, dr \qquad (36)$$

It must be underlined that, in this framework, dynamical effects are not taken into account. It has been shown,[40] using

a Brownian dynamics simulation, that these effects are likely to be very small as compared to the main effect.

In the absence of salt and for trace amounts of reactants, one may insert eqn. (2) into eqn. (35). This leads to the classic (and explicit) result[19]

$$L_0 = \lambda_{AB}/[\exp(\lambda_{AB}\sigma_R^{-1}) - 1] \quad (37)$$

in which λ_{AB} is given by eqn. (3).

Another result may be deduced for high amounts of added salt. In this (theoretical) case, L should tend to a limit corresponding to the Smoluchowski value. Indeed, the charges on the reactants would then become totally screened by the salt, and their effective value would reduce to zero. In this case one may take the limit $g \to 1$ in eqn. (36). This leads to

$$L_\infty = \sigma_R \quad (38)$$

and thus

$$L_\infty/L_0 = [\exp(\lambda_{AB}\sigma_R^{-1}) - 1]/(\lambda_{AB}\sigma_R^{-1}) \quad (39)$$

In what follows, we will consider mainly the case

$$\sigma_R = \sigma$$

3.2.2 Results in the DH approximation. For a dilute supporting electrolyte solution, it is well known that another explicit result may be obtained as follows.

When $\kappa\sigma$ is much smaller than unity one may expand the exponential term in eqn. (5) to the first power in κ. This yields the DH result

$$\beta V_{AB}^{EDH} \sim \lambda_{AB}\left(\frac{1}{r} - \kappa\right)$$

or, by virtue of eqn. (2), (4) and (3),

$$\beta V_{AB}^{EDH} \sim \beta V_{AB}^{(0)} - \lambda_{AB}\kappa$$

Inserting this relation into eqn. (35) leads to

$$L^{EDH_1} = L_0 \exp(\lambda_{AB}\kappa) \quad (40)$$

in which the superscript EDH_1 is used to indicate that an expression at the EDH level was expanded to the first power for κ.

Thus, we get

$$\ln(L^{EDH_1}/L_0) = \lambda_{AB}\kappa \quad (41)$$

which equation, as mentioned in the Introduction, is identical to eqn. (25), established in the case of ACRs.

Let us notice that the formula,

$$\ln(L/L_0) = \lambda_{AB}\kappa/(1 + \kappa\sigma) \quad (42)$$

similar to eqn. (24), has been used[8,12,15,17] in the literature to describe the deviation from simple behaviour, eqn. (41), at higher salt concentrations. However, this formula cannot be derived from eqn. (5), and (35). It was written by analogy with the case of ACRs (eqn. (24)). The validity of eqn. (42) is examined in the following section.

4 Results and discussion

4.1 Determination of ion size for the salt

Best values for the parameter σ_S (the common ionic size) were determined by fitting the MSA estimate of the osmotic coefficient to experimental data at 25 °C, taken from a well-known compilation.[41] This was done by using a theoretical expression for the osmotic coefficient of solution, derived in previous work,[30]

$$\phi = 1 - \frac{\Gamma^3}{3\pi(\rho_+ + \rho_-)}$$

in which Γ is given in eqn. (8).

In the fitting procedure, the size σ_S was taken independent of salt concentration and the permittivity was that of water; experimental data were limited to moderate salt concentration.

The results are summarized in Table 1. One may notice that, in the case of $La(ClO_4)_3$ solution, experimental data for this salt have been described previously[38] without need for the introduction of ion pairing.

4.2 Description of ACRs

First, the EDH and EMSA theoretical results may be compared for typical values of the parameters. For this purpose, let us define

$$D = [\ln(k/k_0)^{EMSA} - \ln(k/k_0)^{EDH}]/\ln(k/k_0)^{EDH} \quad (43)$$

as the relative deviation between the expressions of eqn. (24) and (30).

This quantity is plotted in Fig. 1 for a 1 : 1 salt with $\sigma_S = 4 \times 10^{-10}$ m, for 2 values of the salt concentration, $C_S = 0.1$ and 1 mol dm^{-3}, and for 2 values of the distance of closest approach, $\sigma = 5$ and 8×10^{-10} m. The value of D is computed as a function of s defined by

$$\sigma_A = s$$

$$\sigma_B = 2\sigma - s$$

One observes in Fig. 1 that the EMSA prediction for $\ln(k/k_0)$ is always smaller than the EDH result for these

Table 1 Values for σ_S, the size of ions of the salt

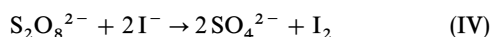| Salt	Max. m^a /mol kg^{-1}	σ_S /10^{-10} m	AARD (%)^b
LiCl	1	3.99	0.3
LiClO$_4$	0.5	4.58	0.3
NaCl	1	3.40	0.3
NaBr	1	3.61	0.3
NaClO$_4$	0.5	3.55	0.2
NaNO$_3$	1	2.73	0.3
Na$_2$SO$_4$	0.5	2.96	1.5
KNO$_3$	0.5	1.85	0.3
BaCl$_2$	0.5	4.17	0.6
La(ClO$_4$)$_3$	0.05	6.07	0.6

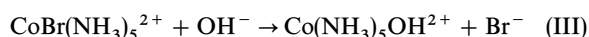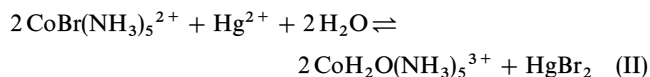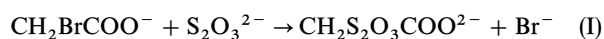^{a} Molality. ^{b} Average absolute relative deviation.
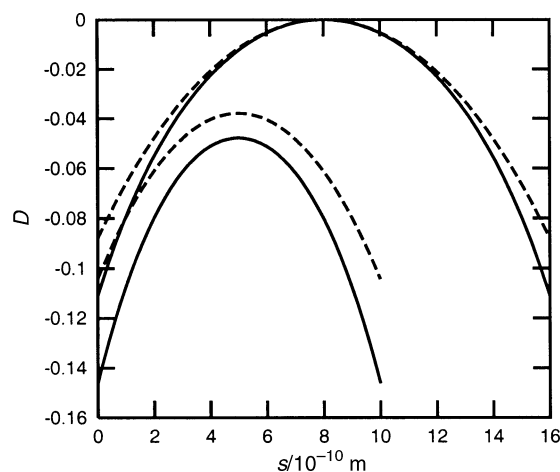
Fig. 1 Plot of D against s (at constant σ) for a 1 : 1 salt with $\sigma_S = 4 \times 10^{-10}$ m. Upper curves: $\sigma = 8 \times 10^{-10}$m, $C_S = 0.1$ mol dm^{-3} (dotted line), $C_S = 1$ mol dm^{-3} (solid line). Lower curves: $\sigma = 5 \times 10^{-10}$ m, $C_S = 0.1$ mol dm^{-3} (dotted line), $C_S = 1$ mol dm^{-3} (solid line).

typical parameter values. In any case, the value of D is smaller than 10% (in absolute value), which deviation is obtained when one of the reactants has a diameter of 2×10^{-10} m. A noticeable result is that D is zero when $\sigma_A = \sigma_B = 2\sigma_S$ (upper curves for $s = 8 \times 10^{-10}$ m), in which case $\ln(k/k_0)_r^{EMSA} = \ln(k/k_0)^{EDH}$, as can be seen in eqn. (33). It is observed that the value of D increases only slightly (in absolute value) with the salt concentration. Moreover, as seen in the restricted case, the discrepancy is larger for smaller reactants.

The compared ability of the EDH and EMSA models to represent experimental data is now examined.

The reactions, and the data for a given reaction, were selected on the basis that the reactant concentration was much smaller than the salt concentration. The following reactions were considered.

$$CH_2BrCOO^- + S_2O_3^{2-} \rightarrow CH_2S_2O_3COO^{2-} + Br^- \quad (I)$$

$$2\,CoBr(NH_3)_5^{2+} + Hg^{2+} + 2\,H_2O \rightleftharpoons$$
$$2\,CoH_2O(NH_3)_5^{3+} + HgBr_2 \quad (II)$$

$$CoBr(NH_3)_5^{2+} + OH^- \rightarrow Co(NH_3)_5OH^{2+} + Br^- \quad (III)$$

$$S_2O_8^{2-} + 2\,I^- \rightarrow 2\,SO_4^{2-} + I_2 \quad (IV)$$

It has been shown that the rate determining step of these reactions is bimolecular[42] with respect to the reacting ions. The kinetic experiments corresponding to reactions (II) and (III) were performed at 15 °C; those for reactions (I) and (IV) were conducted at 25 °C. In all cases, the MSA parameters of Table 1 (for solutions at 25 °C) were taken in this study. In the case of reactions (II) and (III) at 15 °C, the temperature was set to 288.15 K in the MSA equations, which modified the value of λ in eqn. (4).

The theoretical equations corresponding to the EDH and EMSA descriptions (eqn. (24), and (30) or (32), respectively) were fitted to the kinetic data using a Marquardt-type least-square algorithm. Two parameters were adjusted, namely the

kinetic rate without salt, k_0, and one reactant size parameter. The latter is σ in the EDH expression, eqn. (24). For reactions (III) and (IV), the size of the anion was taken from previous work[38,43] for the EMSA description: this led to taking $\sigma_{OH^-} = 3.55 \times 10^{-10}$ m and $\sigma_{I^-} = 4.32 \times 10^{-10}$ m (crystallographic value). For reaction (II), the diameter of Hg^{2+} was estimated to be 6×10^{-10} m on the basis of results for other divalent cations.[43] In these cases, eqn. (30) was used and the size of the other reactant was adjusted. In the case of reaction (I), it was assumed that $\sigma_A = \sigma_B$ and eqn. (32) was employed to fit this parameter.

The results obtained from this procedure are listed in Tables 2 and 3. The adjustment of data using the EMSA expression is presented in Fig. 2 for the case of reactions (I) and (III), for which the maximum ionic strength is in excess of 0.1 mol dm^{-3} (limit of applicability of the EDH description). In Fig. 3 are plotted the curves for reaction (II), including the data for $La(ClO_4)_3$ as the added salt; for this salt, the maximum I is 0.05 mol dm^{-3}, which is also above the limit of the EDH model for this 3 : 1 salt. As seen in Tables 2 and 3, despite this limitation, the EDH representation yields fits of comparable accuracy. However, the EDH and EMSA parameter values are different.

For reaction (III), the data for the 3 salts could be described using common values for k_0 and the reactant size, for both the EMSA and the EDH models. For reaction (IV), the data are well represented with a plausible value for the size of the persulfate ion, $S_2O_8^{2-}$. In the latter case, only the reaction in LiCl was considered because the Li$^+$ cation is expected to lead to the smallest amount of ion association.

In the case of reaction (I), common values were found only for the size parameter. For reaction (II), equal values were obtained for k_0 in the univalent salts. In the latter case, the values for σ_A (A representing the $CoBr(NH_3)_5^{2+}$ ion) in Table 2 are more consistent than those given in Table 3. For both reactions, the kinetic data for a reaction in a given salt could

Table 2 Description of kinetic data using the EMSA model: results for the adjustment of k_0 and reactant size (see text)

Reaction	Ref.	Salt	Max. I^a /mol kg^{-1}	k_0 /mol^{-1} dm^3 s^{-1}	σ_A or σ 10^{-10} m	AARD^b (%)
(I)	c	NaNO$_3$	(I)	4.75×10^{-3}	7.06	1.7
(I)	c	Na$_2$SO$_4$	1.5	3.70×10^{-3}	7.06	3
(II)	c	NaClO$_4$	0.05	1.31	11.1	0.7
(II)	d	KNO$_3$	0.03	1.31	7.54	3
(II)	c	La(ClO$_4$)$_3$	0.05	1.40	8.83	0.6
(III)	d	NaCl	0.03	1.74	3.52	4
(III)	c	NaBr	0.26	1.74	3.52	2.5
(III)	d	BaCl$_2$	0.03	1.74	3.52	3.5
(IV)	e	LiCl	0.1	1.72×10^{-2}	5.40	0.8

^{a} Maximum ionic strength. ^{b} Average absolute relative deviation of fit. ^{c} Ref. 44. ^{d} Ref. 1. ^{e} A. Indelli and J. E. Prue, *J. Chem. Soc.*, 1959, 107.

Table 3 Description of kinetic data using the EDH model: results for the adjustment of k_0 and closest approach distance σ

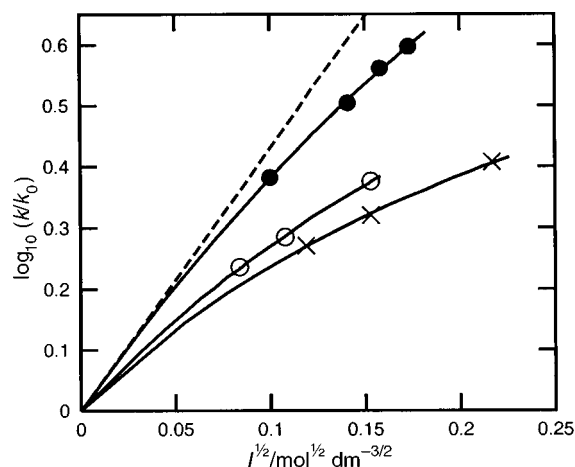| Reaction	Ref.	Salt	Max. I^a /mol kg^{-1}	k_0 /mol^{-1} dm^3 s^{-1}	σ_A /10^{-10} m	AARD^b (%)
(I)	c	NaNO$_3$	1	4.77×10^{-3}	6.86	1.9
(I)	c	Na$_2$SO$_4$	1.5	3.77×10^{-3}	6.86	3.3
(II)	c	NaClO$_4$	0.05	1.31	10.7	0.8
(II)	d	KNO$_3$	0.03	1.31	6.89	2.5
(II)	c	La(ClO$_4$)$_3$	0.05	1.16	13.2	0.7
(III)	d	NaCl	0.03	1.75	4.12	4.5
(III)	c	NaBr	0.26	1.75	4.12	2.4
(III)	d	BaCl$_2$	0.03	1.75	4.12	4
(IV)	e	LiCl	0.1	1.66×10^{-2}	6.45	0.9

^{a} Maximum ionic strength. ^{b} Average absolute relative deviation of fit. ^{c} Ref. 44. ^{d} Ref. 1. ^{e} A. Indelli and J. E. Prue, *J. Chem. Soc.*, 1959, 107.
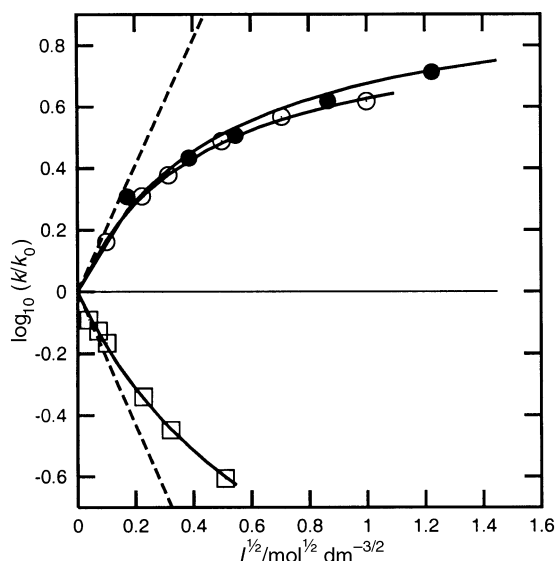
Fig. 2 Plot of $\log(k/k_0)^{EMSA}$ *vs.* $I^{1/2}$. Above the *x*-axis: results for reaction (I) below the *x*-axis: reaction (III). Added salts: Na_2SO_4 (●), $NaNO_3$ (⊙), $NaBr$ (□). Lines: EMSA result (solid line), DHLL result (dashed line).

Fig. 3 Plot of $\log(k/k_0)^{EMSA}$ *vs.* $I^{1/2}$, for reaction (II). Added salts: KNO_3 (●), $NaClO_4$ (⊙), $La(ClPO_4)_3$ (×). Lines: EMSA result (solid line), DHLL result (dashed straight line).

be represented with realistic parameter values. However, the lack of consistency observed for the sets of parameter values suggests that additional phenomena (such as ion association or ionic catalysis) are likely to play a role.[42,44]

Summarising these results, the EDH and EMSA may be used to represent the experimental data. Above 0.1 mol dm^{-3}, the values of the parameters used for the EDH model differ from those for the EMSA but both descriptions are nearly equally satisfactory.

4.3 Description of DCRs

First, the theoretical results for the quantity L were compared with one another. L is given by eqn. (35) in which the EDH or EMSA PMFs (eqn. (5) or (20), respectively) may be inserted. For given conditions, the EDH and EMSA values for $\ln(L/L_0)$ were computed numerically using the Maple™ computation system. The values of L^{EMSA} were computed by including terms up to $n = 4$ for the series in eqn. (20).

Table 4 gives the results for $\ln(L/L_0)$ with these two approaches, and the result from eqn. (42), at 25 °C. The computation of these quantities was extended up to an ionic strength of 4 mol dm^{-3}. (As noticed above, in the present version of the MSA (eqn. (7)), the effect of a salt depends on

Table 4 Comparison of results for DCRs: EDH and EMSA results, and result from eqn. (42). For all data: $z_+ = -z_- = 1$ (for the salt), and $\sigma_A = 6 \times 10^{-10}$ m, $\sigma_B = 4 \times 10^{-10}$ m (so that $\sigma = 5 \times 10^{-10}$ m), $z_A = +1$, $z_B = -1$ (for the reactants). For a given salt concentration, in the column for EMSA, the first line corresponds to a size for the salt ions $\sigma_S = 3 \times 10^{-10}$ m, the second line to $\sigma_S = 4 \times 10^{-10}$ m, and the third line to $\sigma_S = 5 \times 10^{-10}$ m

I^a /mol dm^{-3}	κ /10^{10} m^{-1}	$\ln(L^{EDH}/L_0)$	$\ln(L^{EMSA}/L_0)$	RD^b (%)	Eqn. (42)
0.01	0.032 89	−0.1611	−0.1593	1.1	−0.2018
			−0.1585	1.6	
			−0.1577	2.1	
0.05	0.073 53	−0.2752	−0.2714	1.4	−0.3842
			−0.2678	2.7	
			−0.2649	3.7	
0.1	0.1040	−0.3327	−0.3271	1.7	−0.4889
			−0.3223	3.1	
			−0.3182	4.3	
0.5	0.2325	−0.4638	−0.4548	1.9	−0.7684
			−0.4470	3.6	
			−0.4403	5	
1	0.3289	−0.5110	−0.5008	2	−0.8887
			−0.4928	3.6	
			−0.4859	4.9	
2	0.4651	−0.5491	−0.5393	1.8	−0.9994
			−0.5316	3.2	
			−0.5244	4.5	
3	0.5696	−0.5671	−0.5572	1.7	−1.058
			−0.5502	3	
			−0.5437	4.1	
4	0.6577	−0.5779	−0.5685	1.6	−1.096
			−0.5621	2.7	
			−0.5556	3.9	
" + ∞ "	" + ∞ "	−0.6309^c	−0.6309^c	0	−1.429

^{a} Ionic strength. ^{b} Relative deviation between EDH and EMSA results (preceding two columns). ^{c} Theoretical limit found from eqn. (39).

the values of ionic strength I and on σ_S. This is why the first column of Table 4 is I.) The calculations were performed for reactants of sizes $\sigma_A = 6 \times 10^{-10}$ m and $\sigma_B = 4 \times 10^{-10}$ m, that may be characteristic values for a fluorescence quenching reaction, and for reactant charges $(z_A, z_B) = (+1, -1)$. These values yield $\sigma = 5 \times 10^{-10}$ m using eqn. (14). The effect of the nature of the salt was studied by considering 3 values for σ_S, namely 3, 4 and 5×10^{-10} m. The value of the theoretical limit, found using eqn. (39), is also given in this table.

It is observed in Table 4 that the EMSA result varies slightly with the size of the salt ions. However, the deviation between the EMSA and EDH results increases with the value of σ_S. Nevertheless, the agreement between the two is rather good in all cases. It was found also that these quantities are very close for reactants having valences $z_A = +2$ and $z_B = -1$ (results not shown). Moreover, the MSA result was found to be almost independent of the size asymmetry between the reactants.

The closeness observed between the EDH and EMSA results, even above 0.1 mol dm^{-3}, may be explained as follows. At low ionic strength, the values of the corresponding RDFs, appearing in eqn. (36), are identical. As the ionic strength is increased, the two RDFs deviate more and more, but this deviation is very short ranged. This may be seen in Fig. 4, in which the RDFs are plotted against r for the conditions of Table 4, for a size $\sigma_S = 5 \times 10^{-10}$ m and an ionic strength of 2 mol dm^{-3}. It is noticed on this plot that $g^{EMSA} \simeq g^{EDH} \simeq 1$ for $r \geqslant \sigma + \sigma_S$ (1 nm here). Thus, the range of the deviation between the EMSA and EDH RDFs is of the order of 1 salt ion diameter. In Fig. 4, the largest deviation is for $r \simeq 6 \times 10^{-10}$ m where its value is $ca.$ 8%. The EMSA and EDH plots for the function

$$h(r) \equiv \sigma^2/[r^2 g_{AB}(r)]$$

are shown in Fig. 5 for the same parameter values and the same ionic strength, together with the functions $h_0(r) \equiv \sigma^2/[r^2 g_{AB}^{(0)}(r)]$ (absence of salt) and $h_\infty(r) \equiv \sigma^2/r^2$ (excess of salt). The curve for h for a finite salt concentration lies between h_0 and h_∞. Fig. 5 shows that, although an appreciable discrepancy between h^{EMSA} and h^{EDH} exists in the region near contact, its influence on the value of L (eqn. (36)) is reduced because the two functions are equal long before h reaches zero (in eqn. (36) the integration is performed between σ and $+\infty$). Numerically, for the same conditions, one finds that the EMSA and EDH integrals of h between σ and $\sigma + \sigma_S$ differ by $ca.$ 6%; when the integrals are computed between σ and $+\infty$ this difference reduces to $ca.$ 2%. Notice that, in the fifth
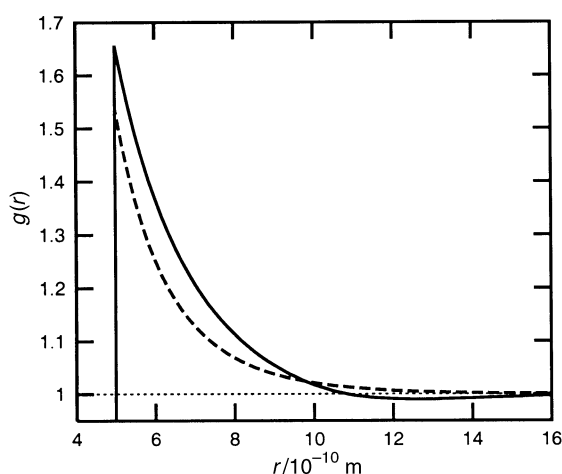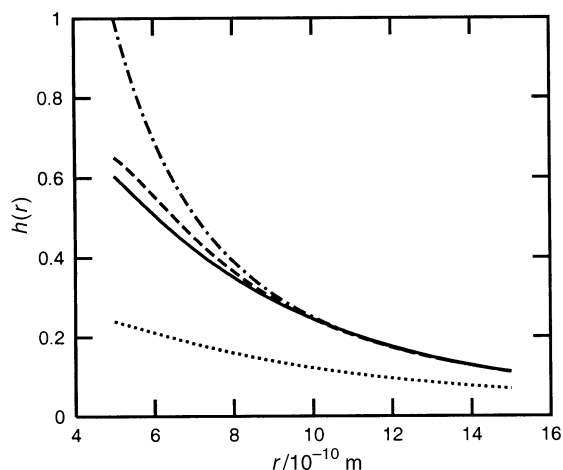
Fig. 5 Plot of $h(r) \equiv \sigma^2/[r^2 g_{AB}(r)]$: EMSA result (solid line), EDH result (dashed line), absence of salt ($h_0(r)$, dotted line), excess of salt ($h_\infty(r)$, dash-dotted line).

column of Table 4, the relative deviation (RD) between the EMSA and the EDH estimate for $\ln(L/L_0)$ is larger than that for L because, symbolically

$$RD \equiv \frac{\Delta \ln(L/L_0)}{\ln(L/L_0)} \simeq \frac{\Delta L/L}{\ln(L/L_0)}$$

in which Δ represents the deviation, and $\ln(L/L_0)$ is smaller than unity in the present case. For the same reason, the relative deviation for $\ln(L/L_0)$ has a maximum near $I = 0.5$ mol dm^{-3}, while that for L increases monotonically with I.

It is interesting to note that if $\sigma_R > \sigma$ then the EDH and EMSA results are still closer. In the case that $\sigma_R > \sigma + \sigma_S$, Fig. 5 shows that the two results will be hardly distinguishable.

Furthermore, the results of Table 4 show that the value of $\ln(L/L_0)$ is not very sensitive to the nature of the salt, as characterised here by the size of the salt ions. This conclusion is in accord with experimental observations.[8,9,11]

One notices in Table 4 that the use of eqn. (42) (last column of Table 4) in this context yields inaccurate results, except at very low concentrations that are not used in practice. Let us introduce the size parameter σ' such that

$$\ln(L^{EDH}/L_0) = \lambda_{AB}\kappa/(1 + \kappa\sigma')$$

Then, using the results of Table 4, and results for reactants of charges $z_A z_B = \pm 2$ and the same size $\sigma_A = \sigma_B = 5 \times 10^{-10}$ m in the same supporting electrolyte, we get values for σ' that are plotted in Fig. 6. One notices that the σ' values are greater than the common reactant size by a factor between 2.2 and 3.8 in the salt concentration range $C_S = 0.01$–4 mol dm^{-3}. This plot suggests that a fit of experimental data using eqn. (42) may yield closest approach distances for the reactants that are significantly greater than the 'true' value.

Lastly, the theoretical results were applied to represent data obtained in a water radiolysis experiment.[15] We considered the two reactions

$$H_3O^+ + H_2O^- \rightarrow H + 2 H_2O \qquad \text{(v)}$$

$$H_2O^- + NO_2^- \rightarrow NO_2^{2-} + H_2O \qquad \text{(vi)}$$
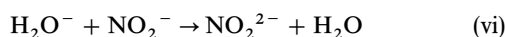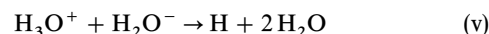
for which LiClO$_4$ was the added salt. In these equations, H$_2$O$^-$ denotes the solvated electron, produced by water radiolysis.

A peculiarity has been demonstrated[15] for these reactions that allowed the determination of experimental values for the
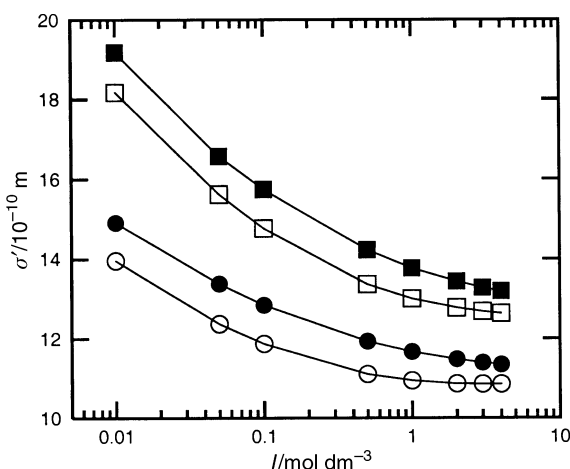
Fig. 4 Plot of $g_{AB}(r)$ for the system considered in Table 4 with $\sigma_S = 5 \times 10^{-10}$ m and $C_S = 2$ mol dm^{-3}. EDH result (dotted line); EMSA result (solid line).

Fig. 6 Plot of σ' values. Case $z_A = +2$, $z_B = -1$: EMSA result (black square), EDH result ($\square$); Case $z_A = +1$, $z_B = -1$: EMSA result ($\bullet$), EDH result ($\odot$).

ratio k/k_0. Therefore k_0 need not be adjusted in this case, which reduces the number of unknown parameters. This feature is interesting since the parameters need be determined manually by computing at each step the numerical value of L through eqn. (35).

The data could be fitted using the EMSA expression for $\ln(L/L_0)$, by assuming that the diffusion coefficient of the species does not vary with salt addition. The adjustment led to the following values: $\sigma_{H_3O^+} = \sigma_{H_2O^-} \simeq 10^{-10}$ m, and $\sigma_{NO_2^-} \simeq 4 \times 10^{-10}$ m. So these reactions are examples of situation in which the size of the reactants is smaller than that of the salt.

The result of the fitting procedure using the EMSA expression is shown in Fig. 7, together with those from the EDH equation, from eqn. (42) with the same values for σ, and from
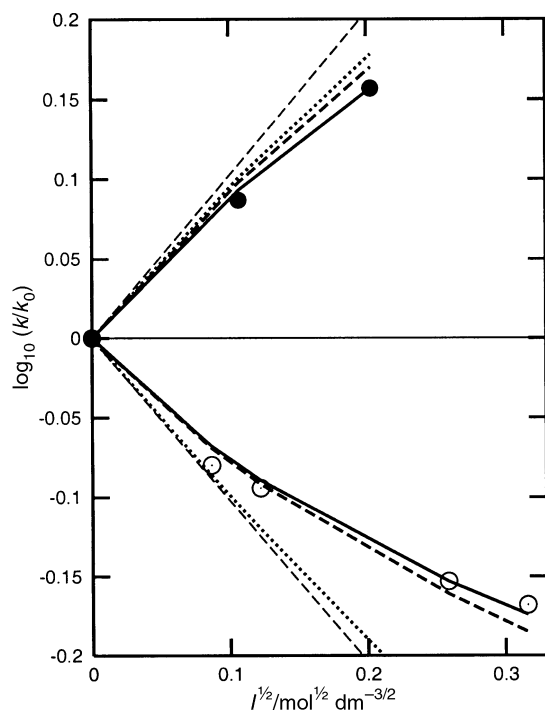

Fig. 7 Adjustment of data for water radiolysis experiment using the EMSA expression (solid line). The other curves are the results with the same parameter values for EDH formula (dashed line), eqn. (42) (dotted line) and eqn. (40) (straight dashed line).

eqn. (40). The EMSA and EDH curves are close to each other. The result obtained using eqn. (42) is fair for reaction (VI) but is quite bad for reaction (V).

In the original work,[15] the kinetic salt effects for reactions (V) and (VI) were described empirically using an equation of the form $I^{1/2}/(1 + I^{1/2})$. In comparison, the present description provides a satisfactory theoretical basis, yielding reactant sizes that have plausible magnitudes.

Thus, the main conclusion that may be drawn in the case of DCRs is that the EDH description gives results that are quite close to the EMSA results, for the same parameter values. This finding may help in understanding the experimental observation that the kinetic salt effect on a DCR does not seem to depend much on the nature of the added salt, for a given ionic strength.

In subsequent work, the interpretation of other experimental data will be attempted in the light of these results.

Acknowledgements

References

1 J. N. Brönsted and R. Livingston, *J. Am. Chem. Soc.*, 1927, **49**, 435.
2 P. Debye and E. Hückel, *Phys. Z.*, 1923, **24**, 185 and 305.
3 R. Livingston, *J. Chem. Educ.*, 1930, **7**, 2887.
4 P. Langevin, *Ann. Chim. Phys.*, 1903, **28**, 433.
5 P. Debye, *Trans. Electrochem. Soc.*, 1942, **82**, 265.
6 R. W. Stoughton and G. K. Rollefson, *J. Am. Chem. Soc.*, 1939, **61**, 2034.
7 J. Q. Umberger, *J. Am. Chem. Soc.*, 1945, **67**, 1099.
8 W. E. Harty and G. K. Rollefson, *J. Am. Chem. Soc.*, 1954, **76**, 4811.
9 F. Tanaka, T. Ishibashi and M. Okamoto, *J. Photochem. Photobiol A*, 1993, **74**, 15.
10 M. E. Morrison, R. C. Dorfmann and S. E. Webber, *J. Phys. Chem.*, 1996, **100**, 15187.
11 B. Verity and S. W. Bigger, *Int. J. Chem. Kinet.*, 1996, **28**, 919.
12 S. W. Bigger, P. J. Watkins and B. Verity, *Int. J. Chem. Kinet.*, 2000, **32**, 473.
13 M. Mac and B. Tokarczyk, *Chem. Phys. Lett.*, 1999, **304**, 309.
14 Y. Yokoyama, M. Moriyasu and S. Ikeda, *J. Inorg. Nucl. Chem.*, 1976, **38**, 1329.
15 G. Czapski and H. A. Schwarz, *J. Phys. Chem.*, 1962, **66**, 471.
16 F. Barat, L. Gilles, B. Hickel and B. Lesigne, *J. Phys. Chem.*, 1973, **77**, 1711.
17 C. D. Jonah, J. R. Miller, E. J. Hart and M. S. Matheson, *J. Phys. Chem.*, 1975, **79**, 2705.
18 B. Hickel, *J. Phys. Chem.*, 1978, **82**, 1005.
19 J. I. Steinfeld, J. S. Francisco and W. L. Hase, in *Chemical Kinetics and Dynamics*, Prentice-Hall, Upper Saddle River, NJ, 1999.
20 R. E. Weston and H. A. Schwarz, in *Chemical Kinetics*, Prentice-Hall, Englewood Cliffs, NJ, 1972.
21 G. Scatchard, *J. Am. Chem. Soc.*, 1930, **52**, 52.
22 W. R. Fawcett, A. C. Tikanen and D. J. Henderson, *Can. J. Chem.*, 1997, **75**, 1649.
23 J. K. Percus and G. Yevick, *Phys. Rev.*, 1964, **118**, 290.
24 J. L. Lebowitz and J. K. Percus, *Phys. Rev.*, 1966, **144**, 251.
25 L. Blum, *Mol. Phys.*, 1975, **30**, 1529.
26 T. Vilariño, P. Alonso, X. L. Armesto, P. Rodriguez and M. E. Sastre de Vicente, *J. Chem. Res. (S)*, 1998, **9**, 559.
27 L. Blum, *Theoretical Chemistry: Advances and Perspectives*, Academic Press, New York, 1980, vol. 5, p. 1.
28 R. A. Robinson and R. H. Stokes, *Electrolyte Solutions*, Butterworths, London, 1959.
29 H. C. Andersen, D. Chandler and J. D. Weeks, *J. Chem. Phys.*, 1972, **57**, 2626.
30 L. Blum and J. S. Høye, *J. Phys. Chem.*, 1977, **81**, 1311.
31 H. C. Andersen and D. Chandler, *J. Chem. Phys.*, 1972, **57**, 1818.
32 S. Hudson and H. C. Andersen, *J. Chem. Phys.*, 1974, **60**, 2188.
33 M. Abramovitz and I. A. Stegun, *Handbook of Mathematical Functions*, Dover, New York, 1972.

34 D. Henderson and W. R. Smith, *J. Stat. Phys.*, 1978, **19**, 191.
35 K. J. Laidler, *Chemical Kinetics*, Harper Collins, New York, 1987.
36 B. Bhalachandra, H. Friedman and M. D. Newton, *J. Chem. Phys.*, 1982, **76**, 1490.
37 S. R. Logan, *Trans. Faraday Soc.*, 1967, **63**, 3004.
38 J. P. Simonin, O. Bernard and L. Blum, *J. Phys. Chem. B*, 1998, **102**, 4411.
39 O. Bernard and L. Blum, *J. Chem. Phys.*, 1996, **104**, 4746.

40 S. Sridharan, J. A. McCammon and J. B. Hubbard, *J. Chem. Phys.*, 1989, **90**, 237.
41 W. J. Hamer and Y. C. Wu, *J. Phys. Chem. Ref. Data*, 1972, **1**, 1047.
42 C. W. Davies, *Progress in Reaction Kinetics*, ed. G. Porter, Pergamon Press, Oxford, 1961, vol. 1.
43 J. P. Simonin, *J. Phys. Chem. B*, 1997, **101**, 4313.
44 A. R. Olson and T. R. Simonson, *J. Chem. Phys.*, 1949, **17**, 1167.